

N65-29815

NASA TMX-55248

FACILITY FORM 8025

(ACCESSION NUMBER)	(THRU)
20	1
(PAGES)	(CODE)
	17
(NASA CR OR TMX OR AD NUMBER)	(CATEGORY)

FE-NI PHASE DIAGRAM

BY
J. I. GOLDSTEIN
R. E. OGILVIE

GPO PRICE \$ _____

CFSTI PRICE(S) \$ _____

Hard copy (HC) 1.00

Microfiche (MF) .50

ff 653 July 65

MARCH 1965



GODDARD SPACE FLIGHT CENTER
GREENBELT, MARYLAND

Fe-Ni Phase Diagram

J. I. Goldstein

and

R. E. Ogilvie

ABSTRACT

29815

The α and γ solubility limits in the Fe-Ni phase diagram have been redetermined at temperatures above 500°C. Both a diffusion couple and a quench-and-anneal technique were used. The solubility limits were measured with an electron probe microanalyzer.

The Ni concentration at the $\gamma/\alpha\gamma$ phase boundary is increased below 700°C and the α solid solubility range is much larger than had been previously measured. The solubility limits were also extrapolated to 300°C. It is suggested that the $\alpha/\alpha\gamma$ boundary bends back to lower Ni contents above 400°C.



J. I. Goldstein, Junior Member AIME, Metallurgist, Theoretical Division, NASA - Goddard Space Flight Center.

R. E. Ogilvie, Associate Professor, Metallurgy Department, Massachusetts Institute of Technology.

The equilibrium diagram has been of great use in the field of meteoritics, where the phase relations between kamacite (α) and taenite (γ) in metallic meteorites can be described by means of the Fe-Ni diagram. The study of metallic meteorites by electron probe microanalysis has cast some doubt on the accuracy of the presently available Fe-Ni diagrams^{1,2}. Recent thermodynamic studies of the Fe-Ni system also suggest that the diagram may be in error³. For these reasons the high temperature (800-500°C) part of the diagram was redetermined.

INTRODUCTION

The currently accepted Fe-Ni diagram is that of Owen and Liu⁴ (Figure 1). Above 910°C, there is a region of complete solid solubility, γ (fcc). Below 910°C, the α (bcc) phase is stable in pure Fe. The effect of increasing amounts of Ni is to stabilize the γ phase. The phases that form when Fe-Ni alloys are heated or cooled bear little relation to the equilibrium diagram. If an alloy is cooled from the γ state and held at a temperature within the $\alpha+\gamma$ field, no evidence has been found for the occurrence of the $\gamma\rightarrow\alpha$ transformation.⁵ If the alloy is cooled to low enough temperatures the γ phase breaks down into a supersaturated bcc phase called α_2 . In fact, in alloys over 27% Ni the γ phase is retained at room temperature.⁶ The α_2 phase has the same composition as the original γ . The temperature at which α_2 forms, the M_s temperature, has been determined experimentally.⁷

A state of equilibrium can be approached by cooling below M_s to form α_2 and then reheating the alloy into the two phase region of the diagram. The γ phase will then begin to precipitate out of the α_2 phase and grow. The growth of the phase, however, is quite slow. Using the

interdiffusion coefficients \bar{D}_α of Goldstein, et al.⁸, it is estimated that it takes about 1 year to grow a 10 micron wide region of γ at 700°C in a 5% Ni alloy.

Owen and Liu⁴ used the technique just described to form the equilibrium phases. The phases present were determined by means of X-ray analysis. The accuracy of their diagram depends on the number of alloys available near the phase boundary at a given temperature.

In this study two different techniques were used to determine the $\alpha/\alpha+\gamma$ and $\gamma/\alpha+\gamma$ solubility limits. The inherent accuracy of both techniques was greatly improved over that used by previous investigators because the phase boundary compositions were measured with an electron-probe microanalyzer.

PROCEDURE

The two methods used to determine the Fe-Ni diagram are the diffusion couple (D.C.) and the quench-and-anneal (Q. + A.) techniques. In the first method, diffusion couples whose diffusion path goes through a two phase region of the phase diagram were used. A description of the technique used for making the diffusion couples has been described in a previous paper.⁸ After the diffusion treatment a discontinuity in the resultant concentration versus distance profile was measured. The Ni concentrations in the α and γ phases at the interface of the discontinuity are the solubility limits of the α and γ phases in the phase diagram at the diffusion temperature. If the interface compositions can be resolved by the probe, then the phase diagram can be determined.⁹ In the Fe-Ni system, it is possible to determine the $\alpha/\alpha+\gamma$ and the $\gamma/\alpha+\gamma$ solid solubilities by this method down to 500°C.

In the second method, an alloy is first cooled from the γ phase to room temperature where α_2 is formed. Then the alloy is annealed in the two phase region of the phase diagram where the γ phase precipitates and grows. If the resultant γ phase is of sufficient size ($>5\mu$), its composition and the interface composition of the α phase can be measured with the electron probe. These compositions are, therefore, the phase boundary compositions of the equilibrium diagram. Figure 2 shows an example of a two phase alloy after the annealing treatment. Nucleation of γ appears to occur at the grain boundaries.

The annealing temperatures, annealing times, and the alloys used for both techniques are listed in Tables I and II. The 800°C diffusion couple was annealed in a high temperature furnace at a vacuum of better than 10^{-5} mm Hg. The other diffusion couples as well as the quenched alloys were sealed in vycor tubes under a vacuum of 10^{-4} mm Hg and annealed in tube furnaces. The temperature control in both types of furnaces was better than $\pm 2^\circ\text{C}$ at temperature.

Before electron-probe microanalysis, these specimens were carefully polished through $\frac{1}{4}$ μ diamond paste. Special care was used so that there were no apparent height differences between the α and γ phases. Areas of interest were identified with microhardness marks.

An ARL (Applied Research Laboratories) electron-beam microanalyzer was used to measure the composition gradients. All data were taken at 30kv with a specimen current between .035 and .05 microamps. Both the NiK_α and the FeK_α radiation were measured. The Fe-Ni calibration curve was determined with 9 Fe-Ni alloys and has already been described.⁸ The calculation of composition from measured X-ray data was greatly simplified

by using the algebraic function A_{ab} developed by Ziebold and Ogilvie¹⁰. This function fits the entire experimental calibration curve by means of a single conversion parameter. The relation between the measured intensity ratio K_A and composition C_A for a binary system is

$$\left(\frac{1-K_A}{K_A}\right) = A_{ab} \left(\frac{1-C_A}{C_A}\right),$$

where $K_A = I/I^0)_A$ of element A,

$C_A =$ atomic per cent of element A.

For the Fe-Ni system at 30kv and for a take-off angle, $\theta = 52.5^\circ$; $A_{ab} = 1.158$ for the Ni and $A_{ba} = .847$ for the Fe intensity curves. The accuracy of measurement obtained by this technique was better than 1% (rel.).

In both the diffusion couples and the quenched and annealed alloys the areas of interest were first analyzed qualitatively with the probe using rate meter scans. After at least 3 areas were selected as representative, quantitative measurements using fixed time counting were taken of these areas. The data were compared with standards of the pure elements and several other alloys both before and after each run. The conversion of X-ray intensity to composition was accomplished with the use of Equation 1. The whole conversion process was programmed and run on the IBM-7094 computer.

RESULTS

Figure 3 shows the composition versus distance curves determined from the diffusion couple technique and the quench and anneal technique at 700°C. The comparability of the two methods is shown by the excellent

agreement of the values of $C_{\alpha}/C_{\alpha}+C_{\gamma}$. The data obtained from both techniques are summarized in Table III along with the measured values of the Fe-Ni diagram by Owen and Liu⁴.

The new phase diagram proposed from the results of this work is shown in Figure 4. The α solid solubility range is greatly extended at high temperatures. The α and γ solid solubility lines are extrapolated below 500°C and a maximum Ni content of approximately 7 At% Ni is predicted in the α phase at about 450°C. The basis for the extrapolation will be discussed later.

DISCUSSION

The errors inherent in the diffusion couple technique and the quench and anneal technique are much smaller than those of the X-ray technique used by Owen and Liu. The measurement errors given in Table III reflect not the accuracy of probe measurement, 1% rel., but the reproducibility of the measured solubility limits from one area to another in a given sample. Not only are the measurement errors small but the results of the two techniques are compatible for the same temperature. Measurements by Winchell¹¹ of $C_{\alpha}/C_{\alpha}+C_{\gamma}$ at 700°C also indicate that considerably more nickel is soluble in alpha-iron-nickel alloys than indicated by the presently accepted diagram.

The uncertainty in the determination of the Owen and Liu diagram cannot be attributed to any lack of sensitivity in the X-ray method used. The uncertainty is due to the difference in Ni content between the two alloys which bracket the solubility limits of the α or γ phase. For example, in determining the $\alpha/\alpha+\gamma$ boundary, one alloy is found to be a mixture of $\alpha+\gamma$ and the other alloy is all α phase. The boundary lies

between these two limits, and the uncertainty is the composition difference between the alloys. Figure 5 shows a comparison of the new diagram and the Owen and Liu diagram. The uncertainties in the determination of both the phase boundaries is also shown. The results of this study fall with the experimental limits of Owen and Liu's work at all temperatures except at 700°C.

According to Owen and Liu's paper: ". . . the phase boundaries determined by this method of surveying structure spectra will need adjustment not exceeding 0.5 At%, the γ phase boundary having a slightly larger Ni content, and the α phase boundary having a slightly higher iron content . . ." This statement is in agreement with our findings on the γ phase boundary and the extrapolated α phase boundary below 500°C.

The diagram below 500°C was not determined in this study because the composition gradients obtained could not be resolved by the electron probe, even if the alloys were annealed for periods of more than 1 year. Attempts have been made by other workers to obtain the solubility limits of α and γ below 500°C. Theoretical calculations have been made by Jones and Pumphrey⁶ and Kaufman and Cohen⁷. Jones and Pumphrey calculated the $\alpha/\alpha+\gamma$ boundary by assuming $\Delta H^{\alpha-\gamma}$ (the difference between the heats of solution of Ni in α and γ iron) independent of temperature and composition. They found that the $\alpha/\alpha+\gamma$ boundary had a maximum Ni content at 400°C and bent back to smaller amounts of Ni content at lower temperatures. This calculation has been criticized by Kaufman and Cohen who state that it is unwarranted to assume $\Delta H^{\alpha-\gamma}$ is completely independent of temperature and composition. Kaufman and Cohen calculated that the bending back of the $\alpha/\alpha+\gamma$ boundary occurred at about 130°C. This calculation was based on the assumptions that the γ solid solution was regular and that the Owen

and Liu diagram gave the correct solubility limits above 350°C.

If one assumes that the bcc (α) solution is ideal at the high iron side of the phase diagram, and that the fcc (γ) solution is a regular solid solution then from equation (13) of Kaufman and Cohen,⁷

$$\Delta F_{Fe}^{\alpha \rightarrow \gamma} = RT \ln \left(\frac{1-C_{\gamma}}{1-C_{\alpha}} \right) - C_{\gamma}^2 B \quad (2)$$

where: $\Delta F_{Fe}^{\alpha \rightarrow \gamma}$ = free energy differences between α and γ phases

C_{α} , C_{γ} = solubility limits in α and γ

B = a function of the heat of mixing H_M^{γ}

Using recent calculations of $\Delta H_{Fe}^{\alpha \rightarrow \gamma}$ ¹² and the measured values of C_{α} and C_{γ} from this work, the above relationship can be used to calculate B as a function of temperature to 500°C.

Using the values of B above 500°C, an extrapolation of B to a temperature as low as 350°C can be made. Using Equation 2 and the extrapolated values of B and C_{γ} , we found that the maximum Ni solubility in α occurs at 450°C. The calculation of C_{α} is strongly dependent on the extrapolated value of B . Because of this, the calculated values of C_{α} below 500°C may be in error by approximately ± 1 At% Ni. The calculated values of C_{α} do however generally follow the extrapolated α solubility curve shown in Figure 4.

Various attempts^{13,14} have been made to produce Fe-Ni alloys in a state of equilibrium at low temperatures by the preparation of fine particles of alloys from the reduction of a salt. In a study of Fe-Ni phase transformations by Kachi, et al.,¹⁴ fine particles of Fe-Ni alloys were obtained by reduction of Fe-Ni oxalates in hydrogen at various

temperatures ranging from 350 to 600°C in less than 25 hours. The amounts of the α and γ phases in the specimens were measured by X-ray diffraction. The results of these studies show an increase in the solubility limit of the α phase down to 350°C. The speed at which equilibrium is said to occur does not allow any growth of α or γ phase by diffusion processes. Because of the small particles sizes used ($<1\mu$) the surface energy may influence the final equilibrium composition of the α and γ phases. Therefore the reported solubility limits may not be representative of equilibrium in bulk alloys.

Owen and Liu state that their measurements indicate that the $\alpha/\alpha+\gamma$ boundary lies between 5.8 and 6.9 At% Ni at 350°C and between 4.8 and 7.5 At% Ni at 300°C. Therefore, since theoretical calculations show that the $\alpha/\alpha+\gamma$ boundary will bend back to lower Ni contents at some temperature below 500°C and the uncertainty of Owen and Liu's diagram below 400°C, it was reasonable to suggest, as did Owen and Sully¹⁵, that the $\alpha/\alpha+\gamma$ boundary bends back to lower Ni contents above 400°C. The actual phase diagram below 500°C, however, is still in doubt.

CONCLUSIONS

The α and γ solubility limits in the Fe-Ni phase diagram have been redetermined at temperatures above 500°C. It was found that with respect to the Owen and Liu diagram;

- (1) The Ni concentration at the $\gamma/\alpha+\gamma$ boundary below 700°C is increased.
- (2) The α solid solubility range is much larger above 500°C.
- (3) The $\alpha/\alpha+\gamma$ boundary probably bends back to lower Ni contents above 400°C.

ACKNOWLEDGMENTS

The authors wish to thank the Smithsonian Astrophysical Observatory for their financial support and for the use of their facilities, and the M.I.T. Computation Center for time on the IBM 7094 computer. The authors would also like to thank Dr. L. Kaufman for his comments and suggestions.

REFERENCES

- ¹S. O. Agrell, J. V. P. Long and R. E. Ogilvie: Nature, 1963, vol. 198, p. 749.
- ²J. I. Goldstein: "Electron Microbeam Probe Studies of Metallic Meteorites," 1962, M. S. Thesis, Massachusetts Institute of Technology.
- ³J. H. Smith, H. W. Paxton and C. L. McCabe: Trans. AIME, 1964, vol. 230, p. 1484.
- ⁴E. A. Owen and Y. H. Liu: J. Iron and Steel Inst., 1949, vol. 163, p. 132.
- ⁵N. P. Allen and C. C. Earley: J. Iron and Steel Inst., 1950, vol. 166, p. 281.
- ⁶F. W. Jones and W. I. Pumphrey: J. Iron and Steel Inst., 1949, vol. 166, p. 121.
- ⁷L. Kaufman and M. Cohen, Trans. AIME: 1956, vol. 206, p. 1393.
- ⁸J. I. Goldstein, R. E. Hanneman, and R. E. Ogilvie - to be published Trans. AIME, vol. 233.
- ⁹R. E. Ogilvie: ScD Thesis, 1955, Massachusetts Institute of Technology.
- ¹⁰T. O. Ziebold and R. E. Ogilvie: Anal. Chem., 1964, vol. 36, p. 322.
- ¹¹P. Winchell: Purdue University, Lafayette, Indiana, private communication.
- ¹²L. Kaufman, E. V. Clougherty, and R. J. Weiss: Acta. Met., 1963, vol. 11, p. 323.
- ¹³F. Lihl: Arch. Eisenhütte, 1954, vol. 25, p. 475.
- ¹⁴S. Kachi, Y. Bando, and S. Higuchi: Jap. Journal of Applied Physics, 1962, vol. 1, p. 307.
- ¹⁵E. A. Owen and A. H. Sully: Phil. Mag., 1939, vol. 27, p. 614.

TABLE I

Alloys for Phase Boundary Determinations

<u>Temperature (°C)</u>	<u>Technique</u>	<u>Alloys</u> (Composition, At% Ni)	<u>Annealing Time</u> (sec)
800	D.C.	0-25.2	2.68×10^6
720	Q+A	5.2	6.05×10^5
700	D.C.	0-15.2	4.85×10^6
700	Q+A	5.2	4.85×10^6
600	D.C.	0-100	1.60×10^7
500	D.C.	0-100	5.25×10^7

D.C. Diffusion Couple Technique

Q+A Quench and Anneal Technique

TABLE II

Chemical Analysis of Fe-Ni Alloys (wt%)

<u>%Ni</u>	<u>%C</u>	<u>%O</u>	<u>N</u> <u>ppm</u>	<u>H</u> <u>ppm</u>	<u>Fe</u>
<0.004	<0.01	0.02	10	<0.5	Remaining
5.17±.02	<0.01	0.02	<10	<0.5	"
15.17±.03	<0.01	0.02	<10	<0.5	"
25.18±.05	0.006	0.02	4	<1.0	"
Remaining	0.001	.006	3	5	5ppm

TABLE III

Composition Limits of the $\alpha+\gamma$ Phases in the Fe-Ni System at 1 Atm.

Temp. ($^{\circ}$ C)	α Solubility (At%)			γ Solubility (At%)		
	C_{α} (meas)	Technique	C_{α} (Owen + Liu)	C_{γ} (meas)	Technique	C_{γ} (Owen + Liu)
800	1.9 \pm .15%	D.C.	1.2%	3.5 \pm .3%	D.C.	3.8
720	3.8 \pm .3%	Q+A	2.2%	8.4 \pm .3%	Q+A	8.2
700	3.9 \pm .2%	D.C.	2.5%			9.4
700	3.9 \pm .2%	Q+A	2.5%	9.4 \pm .2%	Q+A	9.4
600	5.3 \pm .3%	D.C.	3.7%	19.3 \pm .5%	D.C.	7.3
500	6.0 \pm 1.0%	D.C.	5.0%	31.5 \pm .5%	D.C.	27.5

Figure Captions

Figure 1 - Fe-Ni Phase Diagram, Owen and Liu.

Figure 2 - 5.2% Ni Alloy Annealed at 700°C. Two phases - α and γ .
590X, Etchant - 2% Nital.

Figure 3 - Determination of the α and γ Solubilities in the Fe-Ni System
at 700°C (Two Methods).

Figure 4 - Fe-Ni Phase Diagram, Goldstein and Ogilvie.

Figure 5 - Comparison of Fe-Ni Phase Diagrams.

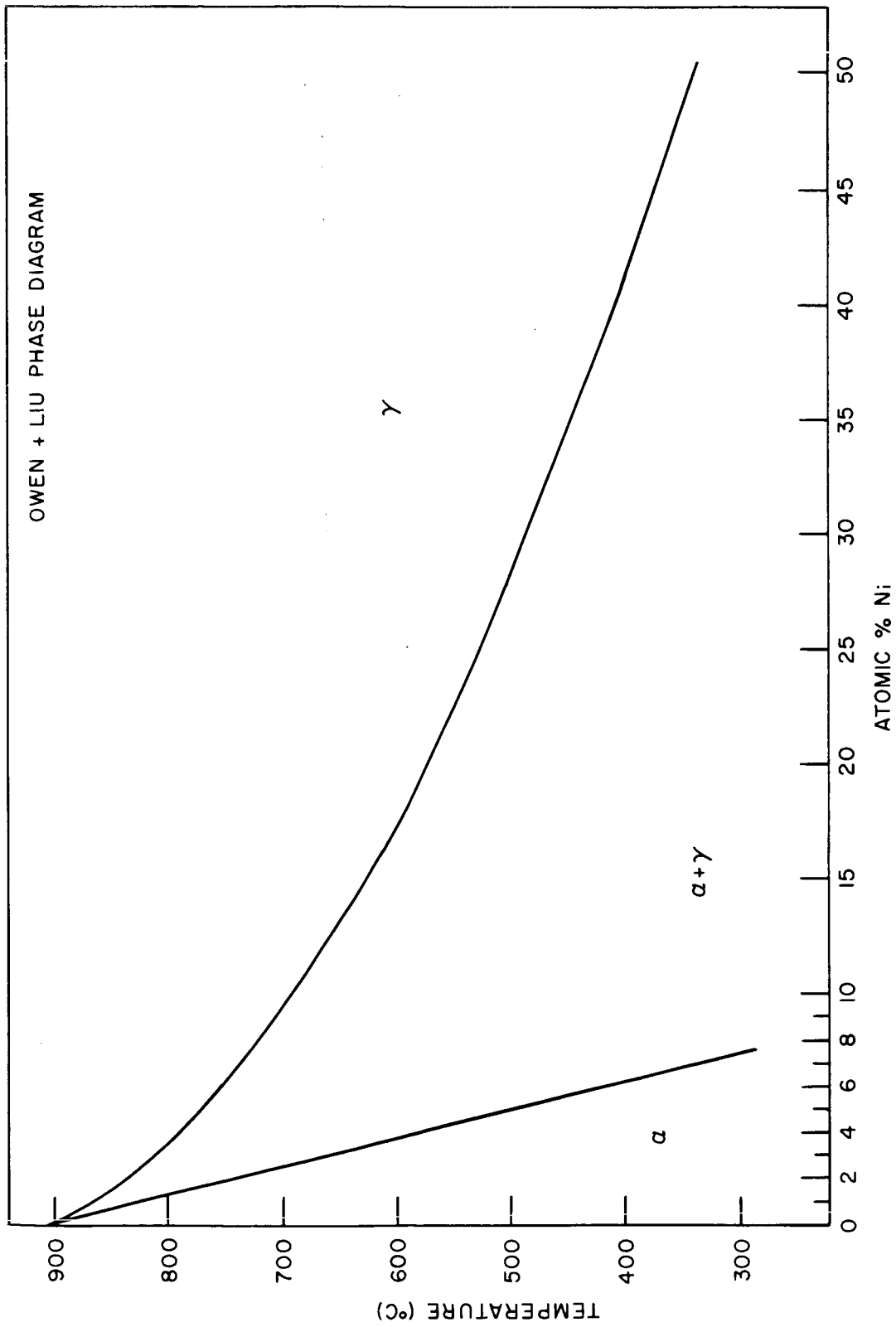


FIGURE 1



FIGURE 2

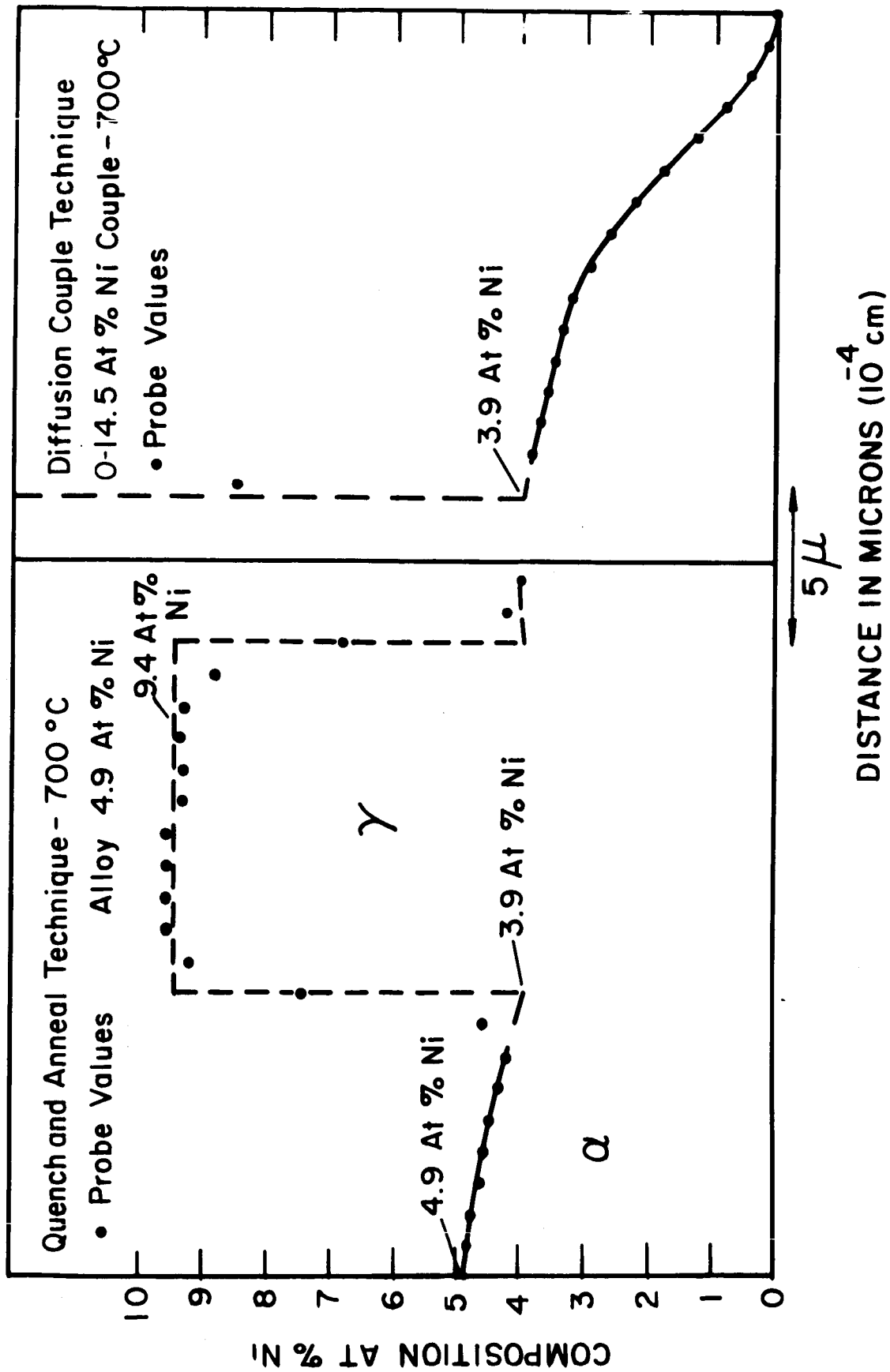


FIGURE 3

